Redox Biology 55 (2022) 102395

Contents lists available at ScienceDirect

Redox Biology

journal homepage: www.elsevier.com/locate/redox

Induction of 2-hydroxycatecholestrogens O-methylation: A missing puzzle piece in diagnostics and treatment of lung cancer

Claudia Musial [a], Narcyz Knap [a], Renata Zaucha [b], Paulina Bastian [a], Giampaolo Barone [c], Giosuè Lo Bosco [d,e], Fabrizio Lo-Celso [f], Lucyna Konieczna [g], Mariusz Belka [g], Tomasz Bączek [g], Antonella Marino Gammazza [h], Alicja Kuban-Jankowska [a], Francesco Cappello [e,h], Stephan Nussberger [i], Magdalena Gorska-Ponikowska [a,c,e,i,*]

[a] Department of Medical Chemistry, Medical University of Gdansk, Debinki 1, 80-211, Gdansk, Poland
[b] Department of Clinical Oncology and Radiotherapy, Medical University of Gdansk, 80-214, Gdansk, Poland
[c] Department of Biological, Chemical and Pharmaceutical Sciences and Technologies, University of Palermo, 90128, Palermo, Italy
[d] Department of Mathematics and Computer Science, University of Palermo, 90133, Palermo, Italy
[e] Euro-Mediterranean Institute of Science and Technology, 90139, Palermo, Italy
[f] Department of Physics and Chemistry 'Emilio Segrè', University of Palermo, 90128, Palermo, Italy
[g] Department of Pharmaceutical Chemistry, Medical University of Gdansk, 80-416, Gdansk, Poland
[h] Department of Biomedicine, Neuroscience and Advanced Diagnostics, University of Palermo, 90127, Palermo, Italy
[i] Department of Biophysics, Institute of Biomaterials and Biomolecular Systems, University of Stuttgart, 70569, Stuttgart, Germany

ARTICLE INFO

Keywords:
Lung cancer
Lung adenocarcinoma
Non-small cell lung cancer
2-Methoxyestradiol
Estrogen metabolites
Biomarker
Blood serum
Molecular modeling
electrophilic potential

ABSTRACT

Lung cancer is one of the most common cancers worldwide, causing nearly one million deaths each year. Herein, we present the effect of 2-methoxyestradiol (2-ME), the endogenous metabolite of 17β-estradiol (E2), on non-small cell lung cancer (NSCLC) cells. We observed that 2-ME reduced the viability of lung adenocarcinoma in two-dimensional (2D) and three-dimensional (3D) spheroidal A549 cell culture models. Molecular modeling was carried out aiming to visualize amino acid residues within binding pockets of the acyl-protein thioesterases, namely 1 (APT1) and 2 (APT2), and thus to identify which ones were more likely involved in the interaction with 2-ME.

Our findings suggest that 2-ME acts as an APT1 inhibitor enhancing protein palmitoylation and oxidative stress phenomena in the lung cancer cell. In order to support our data, metabolomics of blood serum from NSCLC patients was also performed. Moreover, computational analysis suggests that 2-ME as compared to other estrogen metabolism intermediates is relatively safe in terms of its possible non-receptor bioactivity within healthy human cells due to a very low electrophilic potential and hence no substantial risk of spontaneous covalent modification of biologically protective nucleophiles.

We propose that 2-ME can be used as a selective tumor biomarker in the course of certain types of lung cancers and possibly as a therapeutic adjuvant or neoadjuvant.

1. Introduction

Estrogens are enzymatically synthesized from cholesterol. 17β-estradiol (E2) and estrone (E1) are formed by aromatase from testosterone and androstendione, respectively [1]. Their metabolites are being formed in target tissues, and may be either biologically active or inactive. First, E1 and E2 undergo cytochrome CYP450-mediated hydroxylation into their 2, 4, and 16-hydroxy-derivatives. Subsequently, they are metabolized by catechol-O-methyltransferase to their methoxy-derivatives (2-OMEs) [1].

2-Methoxyestradiol (2-ME) is a major metabolite of E2. Interestingly, in contrast to its parent compound, it has potent anticancer and anti-angiogenic activity as confirmed in several *in vitro* and *in vivo* studies [2–7,58]. In our previous research we have established that 2-ME might be potentially used as an effective anticancer agent in therapy of osteosarcoma, neuroblastoma and possibly other solid tumors [6–8]. The

* Corresponding author. Department of Medical Chemistry, Medical University of Gdansk, Debinki 1, 80-211, Gdansk, Poland.
E-mail address: magdalena.gorska-ponikowska@gumed.edu.pl (M. Gorska-Ponikowska).

https://doi.org/10.1016/j.redox.2022.102395
Received 11 May 2022; Received in revised form 15 June 2022; Accepted 2 July 2022
Available online 8 July 2022

therapeutic efficacy of 2-ME (trade name Panzem) has been documented in Phase I and II clinical trials for the treatment of advanced kidney, prostate, ovarian and carcinoid cancers [4,9–17].

In addition, *in vitro* studies have confirmed the antitumor potential of 2-ME in the treatment of breast, colon and lung cancer [18–29]. However, 2-ME did not enter Phase III clinical trials due to the low bioavailability upon oral administration. Therefore, new derivatives and drug formulations of 2-ME are being developed in numerous studies and also by our team.

Despite numerous studies, the detailed mode of anticancer action of 2-ME has not yet been fully elucidated. Previously, we have evidenced that from the mechanistic point of view 2-ME induces the expression and nuclear translocation of the neuronal nitric oxide synthase (nNOS) leading to local nitro-oxidative stress and DNA damage, which ultimately results in death of actively dividing cells or carcinogenesis [2,20]. We have further proved that 2-ME at both physiological and pharmacological concentrations induces mitochondrial fission and mitophagy resulting in BAX activation and osteosarcoma cell death [21].

In our present study we focused on a possible 2-ME-mediated regulation of protein S-palmitoylation as one of the plausible mechanisms of 2-ME anticancer activity. Protein S-palmitoylation is a reversible post-translational modification of protein molecules which alters the localization, stability, and function of hundreds of proteins in the cell [22]. S-palmitoylation is essential for the function of both oncogenes (e.g., NRAS and EGFR) and tumor suppressors (e.g., SCRIB, melanocortin 1 receptor) [23]). In mammalian cells, the removal of palmitate residue is catalyzed by serine hydrolases, including acyl-protein thioesterases (APTs). These enzymes modulate the function of critical oncogenes and tumor suppressors, and often display altered expression patterns in cancer [24].

Notably, targeting S-palmitoylation or the enzymes involved in cellular palmitoylation dynamics may therefore be considered as a potential therapeutic strategy in various types of cancer. Our research has demonstrated that S-palmitoylation serves as a molecular switch regulating the BCL-2-associated X (BAX) trafficking to mitochondria and consequently inducing apoptosis [25]. APT enzymes are soluble, mostly localized in the cytoplasm, and play active roles in maintaining the directional palmitoylation cycle which seems to be of critical importance for the peripheral membrane protein trafficking [25]. However, up to date, a potential role of palmitoylation in the lung cancer has not been established.

Herein, we have focused on lung cancer, as one of the most common causes of cancer-related deaths worldwide [26]. According to the literature, less than half of the reported deaths concern women. This suggests that lung cancer is a far more common cause of female mortality than breast cancer, ovarian cancer, or uterine cancer. As far as the histological characteristic is concerned, lung cancer is typically divided into the small cell lung cancer (SCLC) and non-small cell lung cancer (NSCLC) which can be specifically further subdivided into adenocarcinoma, large cell carcinoma and squamous cell carcinoma [26].

The available data indicate that estrogen receptors (ERs) are expressed in NSCLC cells via both genomic and non-genomic mechanisms. Nevertheless, the role of ERs in the etiopathogenesis as well as progression and prognosis for NSCLC patients is under discussion, and more in-depth research is still necessary. Importantly, certain studies indicate that high expression of the estrogen alpha (ERα) receptors, as well as the estrogen beta (ERβ) receptor are valuable prognostic markers for the lung cancer patients [27,28].

Researchers point out that cellular processes of critical importance like the induction of NSCLC cell proliferation as well as apoptosis, migration and cancer cell invasion can be mediated via ERs. A number of studies show that women suffering from NSCLC have much more promising results in the course of chemotherapy than men with comparable progression of the disease. This observation suggests that cancer responsiveness to treatment and consequently the prognosis is dependent on sex hormones profile. However, it should be emphasized that hormone replacement therapy in NSCLS women, increases the overall mortality [29]. Moreover, it is important to mention that estrogens have been proved to activate proliferation of the lung cancer cells derived from female patients [30].

Clinical diagnosis of the disease at the earliest possible stage is obviously correlating with an increase in the survival rate [24]. Thus, it is so important to search for novel and easily detectable biomarkers of the disease which may help to predict the risk of cancer development or monitor the course of the disease and specifically, cancer responsiveness to therapy [31].

Based on both *in vitro* studies and clinical analyses, we propose that 2-hydroxycatecholestrogens O-methylation seems to be a physiological anticancer protection mechanism, and that 2-ME should be seriously considered as a useful clinical biomarker or a potential therapeutic in patients suffering from NSCLC.

2. Materials and methods

2.1. Reagents and materials

A549 cell line (ATCC® CCL-185™) was kindly offered by the University of Rzeszów, Poland. 2-methoxyestradiol, 2-hydroxyestradiol, supplements and cell culture media were obtained from Sigma Aldrich. Palmostatin B was purchased from Merck Millipore (178501).

The laboratory equipment used at the Department of Medical Chemistry, Medical University of Gdańsk, in order to process blood samples from patients and the control group was bought from Santa Cruz Biotechnology, Inc.

2.2. Cell culture

The A549 two-dimensional cell line were cultured in Nutrient Mixture F-12 Ham medium supplemented with 10% fetal bovine serum (FBS), 100 μg/mL penicillin/streptomycin, and 2 mM L-glutamine (GlutaMAX™). All cells tested negative for mycoplasma and were cultured sequentially. The culture was maintained at 37 °C in an atmosphere containing 5% CO_2. Cell culture density was kept at the maximum of 1×10^4 cells/mL. At least every two days, medium was replaced with the fresh one, and the cells were counted and reseeded to maintain the recommended density.

Before starting experimental procedures, the optimal cell density was determined by sequentially seeding the cells at different concentrations. Next, cellular confluency analysis within 96-well microplates was performed with CytoSMART® Omni apparatus (Omni, CytoSMART; Eindhoven, The Netherlands) allowing for visualization of each and every well. Cell confluence at the beginning of each experiment was ca. 70% which guarantees accuracy and comparability of the obtained results. Importantly, the cells were never taken out of the incubator in order to eliminate a potential thermal shock effect. All samples were monitored in real time with a series of measurements performed at selected time points.

Wild-type human lung epithelial carcinoma, A549 cell line as 3D cell culture spheroids were obtained by plating cells with an average density of 8000 cells/cm^2 in 96-well U-bottom and V-bottom Lipidure® cell culture plates (Amsbio, Abingdon, United Kingdom) coated with phosphorylcholine which is naturally found in cell membranes. Spheroids were grown in Dulbecco's Modified Eagle's Medium/Nutrient Mixture F-12 Ham (DMEM/F12 Medium, Sigma-Aldrich®), supplemented with 10% FBS, 100 μg/mL penicillin/streptomycin, and 2 mM L-glutamine (GlutaMAX ™). Spheroids were maintained in culture medium and passaged at 70% confluence.

2.3. Experimental design – doses and time of incubation

The experimental conditions, such as time and doses, were primarily

established based on our previous research [32–34]. The conditions were subsequently optimized according to lung cancer A549 cell line.

2.4. Cell viability assay (MTT and WST-1 assays)

The analysis was performed as previously described [25,26]. Cells were seeded in a 96-well plate at a density of 1×10^4 cells/well and incubated in Nutrient Mixture F-12 Ham medium supplemented with FBS, antibiotics (penicillin/streptomycin) and amino acid (L-glutamine) at 37 °C for 24 h. After 24-h incubation, cells were treated with estrogen metabolites at various concentrations. Subsequently, after 24-h incubation, the solution of 0.5 mg/mL 3-(4,5-dimethylthiazol-2-cyl)-2, 5-diphenyltetrazolium bromide (MTT) was added onto the 96-well plates. Then the plates were incubated at 37 °C for 2–4 h and 100 μL of dimethylsulfoxide (DMSO) was added to each well on each microplate, and mixed thoroughly on a rocker shaker to dissolve dark blue crystals, which are clearly visible and marked under the microscope. The absorbance was read using a microplate (ELISA) reader at 540 nm wavelength. The experiments were conducted at least three times.

For the 3D culture of A549 cells, WST-1 (Roche Diagnostics, Mannheim, Germany) assay was performed. The assay is based on the cleavage of tetrazoline salt into formazan. This process is mediated by cellular mitochondrial dehydrogenases. The WST-1 assay was specifically selected for the 3D models of A549 cells as it does not involve additional steps such as washing, harvesting, or solubilizing the spheroidal models. A549 cells were plated at a concentration of 8000 cells/cm^2 in a 96-well U-bottom and V-bottom Lipidure® cell culture plates (Amsbio, Abingdon, United Kingdom). Cells were incubated for 72 h at 37 °C and 5% CO_2. Sub Next, 10 μL/well of Cell Proliferation Reagent WST-1 was added and the samples were incubated for 4 h at 37 °C and 5% CO_2. Then plates were put on a shaker for 1 min. The absorbance of the samples was taken against the background of the control as blank, using a microplate (ELISA) reader. According to manufacturer's protocol, the wavelength for measuring absorbance of the formazan product is between 420 and 480 nm. The experiments were conducted at least three times.

The data from the *in vitro* cell culture experiments were presented as the mean percentage (±SE) of at least three replicates of each study. Cytotoxicity was defined as the percentage of viable cells that remain after treatment with estrogen metabolite compounds. Response curves were determined using GraphPad Prism version 9 (GraphPad Software, San Diego, CA, USA).

2.5. Viability assessment of A549 cell line after treatment with 2-ME

Fluorescent staining allows to visualize cells during a period of cell death at the phase of late necrosis when the cytoplasmic membrane permeability has increased enough. Fluorescence amplification is directly caused by PI intercalation with double-stranded DNA. Microscopic images were acquired using the CytoSMART Lux3 fluorescence microscope (Lux 3, CytoSMART, Eindhoven, The Netherlands).

2.6. Molecular modeling

The structure of APT1 and APT2 proteins were taken from the Protein Data Bank with PDB ids of 5SYM and 5SYN, respectively. The missing eight initial amino acid residues were reconstructed using the MODELLER software package [35,36]. The structures of 2-ME complexes with APT1 and APT2 were first modeled through molecular docking calculations, using the Autodock Vina package [37]. The docking box, based on the ligand size and shape, was determined by Autodock Tools [27]. Two model complexed structures were selected for each of the binding complexes and molecular dynamics (MD) simulations were performed as previously reported [7,38,39].

MD simulations were performed using the AMBER99SB-ILDN force field [40] for the protein as implemented in the GROMACS 2020.2 software package [41]. The simulations for various systems were performed using a cubic box of NaCl 150 mM in explicit TIP3P water solution. Periodic boundary conditions were applied. The force field parameter files and initial configuration for the protein were created by GROMACS utilities programs. The force field parameters of 2-ME have been derived from the Merck Molecular ForceField (MMFF), with van der Waals parameters taken from the closest atom type in CHARMM22, through the SwissParam web interface [42]. The equilibration procedure was performed in several steps, starting from an NVT simulation at 300 K with the protein heavy atom positions restrained to equilibrate the solvent around it, followed by a NPT run at 300 K and the pressure at 1 bar, for a 10-ns run. After the equilibration phase, the system was run for at least 400 ns for an NVT production run; the trajectory was saved at a frequency of 10 ps to evaluate dynamical and structural properties. The simulations were always checked versus the root mean square displacement (RMSD) and the energy profile. During the production runs a velocity rescaling thermostat [43] was used for the temperature coupling, with a time coupling constant of 0.1 ps. A Parrinello–Rahman barostat [44] was used for the pressure coupling, with relaxation constant of 1 ps. The equations of motion were integrated through the Leap-Frog algorithm, using a 2 fs time step. The values of cut-offs of the Lennard-Jones and real space part of the Coulombic interactions were set to 10 Å. The Particle Mesh Ewald (PME) summation method [45–49] was used to evaluate the electrostatic interactions, with an interpolation order of 4 and 0.16 nm of FFT grid spacing.

The 2-ME/APT1 and 2-ME/APT2 complexes shown in Fig. 5 have been selected by clustering analysis [33,34] performed using the g_cluster tool implemented in GROMACS package, and following the method previously described [50]. Protein-ligand interactions were found by using the PLIP service [51]. Protein pictures and manipulation were done using Maestro [Maestro, Schrödinger, LLC, New York, NY, 2018, version 11.6.010] and Chimera [52].

2.7. Identification of reactive oxygen species (ROS) signal in 2-ME-treated A549 cells

Intracellular level of ROS was assessed by means of a fluorescence test. The ROS-Glo™ H2O2 Assay from Promega (Mannheim, Germany) was performed in accordance with the manufacturer's instructions. A549 cells were seeded at the density of 10,000 cells/well in a 96-well white cell culture plate with 100 μl of F12 Ham and 10% FBS.

The level of ROS was also measured in the treated cells, control cells, medium alone as well as in the medium with 2-ME without A549 cells according to the experimental design.

The plate was returned to the incubator for 6 h. Subsequently, 100 μl ROS-Glo™ signal detection solution was added to all the wells. The plate was further incubated for 20 min at room temperature, and the luminescence was recorded with the Promega GloMax® Discover luminometer (Mannheim, Germany). Statistical analysis was performed with GraphPad version 9 using the TTEST function (GraphPad Software, San Diego, CA, USA).

The selected concentrations were chosen as representative ones. The use of the ROS-Glo™ Detection Solution allowed for the conversion of a precursor compound to luciferin as well as for the administration of luciferase.

2.8. Study group

This study was approved by the Independent Bioethical Committee for Scientific Research at the Medical University of Gdańsk with the approval number of 666. The study population comprised fully consented patients with newly diagnosed lung adenocarcinoma and healthy volunteers. A written informed consent was obtained from each participant before any study-related procedures were taken. In order to objectively assess a potential correlation between the analyzed factors and clinical results, the study group was narrowed to only patients

presenting with the newly diagnosed lung adenocarcinoma. Adult patients at the age 18 years with newly diagnosed, histologically confirmed lung adenocarcinoma (all stages; TNM classification) were eligible for inclusion. The control group consisted of healthy volunteers. Patients with other histological subtypes and those who have already received oncological treatment such as chemotherapy, radiochemotherapy, surgery, immunotherapy or molecularly targeted therapies were excluded from the study. Exclusion criteria also comprised acute and chronic inflammatory diseases, asthma, allergies, autoimmune diseases, hormone replacement therapy, hormonal contraception, endocrinopathies, chronic steroid use, kidney failure, heart failure, and other malignancies (excluding radically treated early cervical cancer and early skin cancer) potentially affecting the lungs or function of the endocrine system. Analysis of the level of steroid hormones and the level of nitro-oxidative stress in the serum and urine from patients in both study and control groups were performed. In our study, the control group was comprised of healthy volunteers.

2.8.1. The human subjects

The study group included ten female patients, at the median age of 66 years (range 42–86 years) with newly diagnosed medically inoperable, histologically proven lung adenocarcinoma, poorly differentiated in 5 of 10 patients.

We took into account a number of patients with lung cancer - G2 invasive squamous cell carcinoma with phenotype: TTF1-, p40 +, adenocarcinoma TTF1 +, p63-, adenocarcinoma infiltrants predominantly acinar, non-small cell carcinoma with phenotype: p40 +, TTF1 +, CK- 7+, CK 20+ and: low-differentiated squamous cell carcinoma, PDL1 <3%, p63 +, TTF1-, p40 +, EBER- and small groups of low-differentiated lung adenocarcinoma cells with the phenotype: CK AE1/3 +, TTF1 +, p63. All patients underwent radiological assessments (computed tomography (CT), 18-fluorodeoxyglucose positron emission tomography (PET/CT), and magnetic resonance of the brain (MR)) under the institutional standard of care. There were two patients without regional lymph node (LN) involvement (stage T2N0M0), two patients with hilar LN involvement (N1), two patients with mediastinal LN metastases (N2), and four patients with proven distant metastases (T2-4N2-3M1; liver, brain, bones). Comorbidities included chronic obstructive pulmonary disease (COPD) in 5 of 10 patients, diabetes in one of 10 patients, and hypertension in 6 of 10 patients. Two patients were actively smoking at study entry, while all others had a history of smoking – 1.5 to 60-packyears of smoking, median 40-packyears. There was no history of hormone replacement therapy in the whole group. Cancer family history included lung cancer in one patient and breast cancer in another patient. The control group consisted of 10 cancer-free, healthy non-smoker women aged 25 to 65 (median age of 45).

2.8.2. Taking blood serum samples from study participants

Blood samples were collected by qualified medical personnel under careful supervision of the attending physician. On the same day, the obtained material was transported to the Department of Pharmaceutical Chemistry, Medical University of Gdansk and stored under deep freezing conditions at −80 °C until LC-MS/MS analysis.

In order to improve detection, the tested estrogens and their derivatives were subjected to dehydration process, which resulted in an increase in the molecular weight of the monitored ions. As a result, their identification by the mass detector was enhanced, thereby improving the sensitivity of the method, since the analyte signal was increased at the expense of reduced noise signals. The result was a low pg LOD value. The properties of hydroxyl derivatives were also changed from hydrophilic to lipophilic, which enabled the use of a C18 column and perfect separation of the analytes to be determined in reverse phase. Derivatization was performed in a pre-column mode using dansyl chloride as the derating reagent. Due to the short duration of derivatization and mild conditions (30 s, room temperature), it differs from other reagents previously used in the literature. The advantage of the dansyl chloride used in the present work is also easy availability on the market and relatively low cost. Prior to its use, derivatized analytes can be concentrated using, for example, an SPME extraction method. Derivative compounds for the purposes of this project were isolated from the biological matrix using the liquid-liquid extraction technique with the use of an organic solvent - dichloromethane.

Using the optimized and validated LC-MS/MS method, it is possible to determine 13 analytes: estrogens and their hydroxy and methoxy derivatives within 55 min. Obtaining a satisfactory separation of 13 structurally very similar compounds required the use of a very sensitive apparatus - a tandem mass spectrometer with a triple quadrupole analyzer, and the signals were recorded in the MRM post-reaction mode.

The first quadrupole Q1 captures the parent (quasi-molecular) ion m/z appropriate for each analyzed compound, which then enters the Q2 collision chamber. After triggering a collision, the ions fragment and are filtered through the third quadrupole. Each analyte was identified and determined by monitoring the appropriate ion transitions in the MRM follow-up monitoring mode.

Patient samples were analyzed by the proposed LC-MS/MS method in random order to avoid bias.

2.9. Estrogens analysis in blood serum

Whole blood samples were collected in a test tube containing an activator at the Department of Clinical Oncology and Radiotherapy of the University Clinical Center in Gdańsk. In the Department of Medical Chemistry, patients' blood samples were centrifuged for 10 min at 2000–3000 rpm. Subsequently, the obtained serum (supernatant) was transferred to new tubes. During the centrifugation process, the blood clots were removed. Tubes that could not be analyzed immediately were frozen at −80 °C according to the standard protocol. The amount of serum obtained from patients' whole blood depended on the individual hydration status as well as the amount of blood collected in the clinic.

500 μL of blood serum samples were transferred into a 10-mL threaded glass tube. Next, 4 mL of dichloromethane was added, the samples were screwed with caps and placed onto a rotary shaker set at 40 rpm for 30 min. After that, the organic layer was collected and transferred into another glass tube. Then 10 μL of radiolabeled estrogen derivatives with concentration of 1 μg/mL were added and mixed on a single point shaker for 30 s. The prepared sample was placed in a vacuum concentrator at 30 °C and evaporated to dryness within 40 min. The next step was to carry out the derivatization process of the analytes, and hence 100 μL of 0.1 M sodium bicarbonate buffer pH 9.0 and 100 μL of dansyl chloride with the concentration of 1 mg/ml as dissolved in acetone was used as an analogous reagent. The content of the tube was mixed for 30 s on a single point shaker and transferred into a 500 μL Eppendorf vial, and placed in microtitre plate shaker incubator (shaking heating block), where the samples were heated and mixed simultaneously at a temperature 60°C for 5 minutes. The next step was centrifugation at 8000 rpm for 5 min. and 100 uL of the sample prepared in this way, was transferred into a glass insert of of 200 μL volume, which was then placed in an autosampler and subjected to LC-MS/MS analysis under the conditions described below.

2.10. Determination of estrogens and their derivatives in human blood serum by LC-MS/MS technique

After carrying out the derivatization process, estrogens and their derivatives were determined by liquid chromatography technique coupled with tandem mass detection - LC-MS/MS using the LC-MS-8050 model from Shimadzu (Japan). The mass spectrometer was equipped with an electrospray (ESI) ion source and an MS/MS triple quadrupole analyzer. The estrogens were separated on a C18 core-shell column called Poroshell 120, measuring 100 × 3.0 mm; 2.7 μm, reversed phase (RP). A gradient elution was used in the process (Table 1). The mobile phase A consisted of ultrapure water with 0.1% formic acid, while phase

Table 1
Gradient elution conditions.

time, min	% share of phase B
0 → 45	72 → 87
45 → 47	87 → 100
47 → 48	100 → 72
48 → 55	72

B was methanol.

The optimized conditions for the analytical separation of estrogens and their derivatives by LC-MS/MS were as follows:

- sample volume dosed into the column: 3 μL
- total time of a single analysis: 55 min
- volumetric flow rate of the mobile phase over time: 0.3 mL/min
- column thermostating temperature: 40 °C
- temperature within the autosampler chamber: 4 °C
- MS operating mode: positive
- ESI ion source temperature: 300 °C
- temperature of the heating block: 400 °C
- volumetric flow rate of heating gas (nitrogen) per unit time: 10 L/min.
- volumetric speed of drying gas (nitrogen) flow per time unit: 10 L/min.
- volumetric flow velocity of nebulizing (scattering) gas per time unit: 3 L/min.
- temperature of the desolvation line (DL): 250 °C
- voltage applied to the capillary: 3 kV

The developed analytical method was statistically evaluated in terms of specificity, linearity, LOD and LOQ. The specificity was examined by comparing the chromatogram obtained from the sample without standard addition (blank) with the chromatogram of the sample enriched with the standard solutions of estrogens and their derivatives. The lack of interference of the peaks of endogenous substances from the biological matrix with the peaks of the analyzed estrogens confirmed the specificity of the method. The linearity of the methods within the concentration range from 0.1 ng/mL to 50 ng/mL was confirmed on the basis of plotting a directly proportional relationship between nominal analyte concentrations and the ratio of the area under the peak of the test substance to the area of the internal standard peak. Then, the regression equations were calculated using the least squares method, and the numerical values of the determination coefficient R^2 close to the value of 1 are a measure of the degree of correlation of the variables. The limit of quantification was calculated from the signal-to-noise ratio (S/N = 3).

2.11. Computational chemistry analysis of potential non-receptor bioactivity of 2-ME

Computer analysis was performed by computational chemistry methods of possible non-receptor bioactivity of 2-ME as compared to other natural estradiol metabolites in terms of drug safety in the context of potential induction of oxidative stress and/or DNA damage.

Molecular modeling and optimization of the geometry of 17-β estradiol derivatives were performed in the Gaussian 09 program (revision D.01) made available on high-performance computing clusters as part of a grant from the PLGrid academic supercomputer network using quantum-mechanical methods, including the Hartree-Fock (RHF) computational method and density functional theory (DFT).

The optimization of the geometric structure and energy parameters of the studied molecules was performed at the level of the B3LYP density functional with a functional base of 6–31G (d), based on the Koopmans theorem [53] in terms of the density functional theory according to Kohn and Sham [54] using the method described by Parr [55]. The potential reactivity with weak nucleophiles of cytoprotective importance and the tendency to form adducts with DNA nucleophilic amino groups were estimated by calculating the electrophilic potential of estradiol derivatives, including 17-β estradiol, 2-hydroxyestradiol, 2-methoxyestradiol (2-ME), 2,3-estradiol-ortho-benzoquinone and its methine isomer, as well as 4-hydroxyestradiol, 4-methoxyestradiol (4-ME), estradiol-3,4-ortho-benzoquinone, and analogous estrone derivatives. Lipophilicity and polar surface area of estradiol metabolites was evaluated using MarvinSketch 20.21 by ChemAxon (Academic License).

2.12. Statistical analysis

2.12.1. Statistical analysis of in vitro studies

Data were presented as the mean values (±SE) from at least three independent experiments. Data were analyzed performing one-way ANOVA combined with Dunnett's multiple comparison test; *significantly different at $p < 0.01$ versus the control. A representative experiment out of three performed is shown with GraphPad Prism 9.0 software.

2.12.2. Statistical analysis of clinical tests

Statistical analysis was performed using the IBM SPSS Statistics 25 package. Analysis was performed with the Kruskal-Wallis test, which allowed to check whether there are statistically significant differences between individual groups of people. In the case of statistically significant differences, the Games-Howell post-hoc test was used. Such a selection was made based on the fact that the variances in the compared groups of people were not homogeneous, and also due to the relatively low number of people tested.

For comparison of two groups of people, the Mann-Whitney *U* test was used. The analysis of the Spearman correlation allowed to check whether there was a statistically significant relationship between the analyzed variables. Effect size was measured using the eta-square ratio. The following descriptive statistics were used in the analysis: arithmetic mean, median, standard deviation, minimum, maximum, first and third quartile. The p value < 0.05 was adopted as statistically significant.

3. Results

3.1. Formation of A549 cells spheroids

Chemical gradients of nutrients, oxygen and catabolites are unique to the 3D spheroidal cell culture model. It should be emphasized that the cells located on the periphery of spheroids are believed to illustrate the *in vivo* metabolic pattern of active tumor cells. Conversely, the cells located on the inside of spheroids usually undergo a cell death process. The photos of a single spheroid A549 cell line were included in the supplementary file.

3.2. Impact of 2-ME on the viability of 2D and 3D non-small lung cancer A549 cell line models

In order to determine potential anticancer effectiveness of 2-ME in the lung cancer model, A549 cells established in a 2D- and 3D cultures were tested using MTT and WST-1 assays, respectively. The antiproliferative potential of 2-ME was assessed by 24-h treatment of A549 cells in two-dimensional culture with serial dilutions of 2-ME over a concentration range of 0.78 μM–100 μM in two-fold serial dilutions. The viability of A549 cells was lowered down to 64.6% after treatment with 50 μM 2-ME, and to 55.34% % with the concentration of 100 μM 2-ME (Fig. 1A).

3D spheroidal cells of the A549 line, were treated with the same concentrations in a two-fold serial dilution pattern as the two-dimensional cell culture for comparison. However, in order to verify the resistance of the spheroidal cell model, the cells were also treated

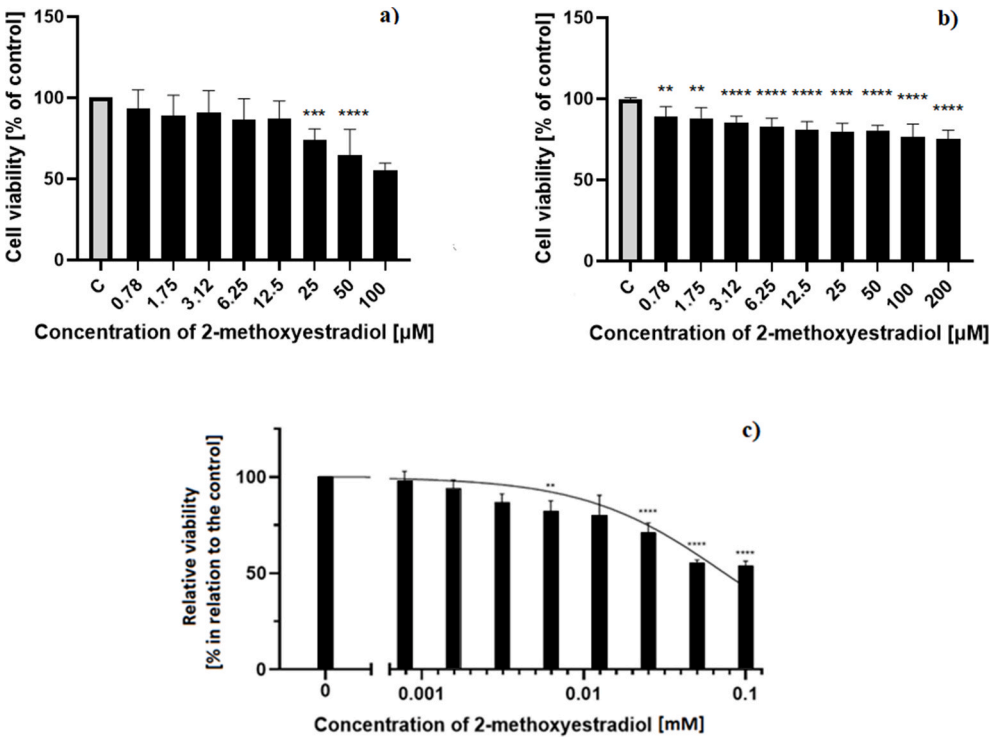

Fig. 1. (A) 2-ME significantly decreases A549 cell viability in a dose-dependent manner in the 2D culture model at concentrations less than or equal 100 μM. A549 cells were treated with serial dilutions of 2-ME at a concentration range from 100 μM to 0.43 μM for 24 h. Cell viability was determined by MTT assay. Presented values are the mean ± SE of three independent experiments. *p < 0.01, **p < 0.001, ***p < 0.0001, ****p < 0.00001 vs. control cells. (B) 2-ME reduces the cell viability of the A549 3D spheroidal models in a dose dependent manner with expenditures close to 200 μM. A549 cells were exposed to serial dilutions of 2-ME over a concentration range of 200 μM–0.78 μM for 48 h. Cell viability was determined by the WST-1 assay. Presented values are the mean ± SE of three independent experiments. *p < 0.01, **p < 0.001, ***p < 0.0001, ****p < 0.00001 vs. control cells. (C) IC50 values for the A549 cell line treated with 2-ME were >100 μM. These values were calculated by analyzing the relationship between concentrations and percentage (%) of inhibition using GraphPad Prism version 9.0 for Windows, GraphPad Software, CA, USA.

with a two-fold higher concentration (200 μM) of estrogen derivative.

The WST-1 proliferation test (Roche Diagnostics, Mannheim, Germany) was performed according to the vendor's protocol. WST-1 was chosen for the spheroidal culture tests because it has a much higher sensitivity and lower cytotoxicity and is stable up to 48 h. The concentration range of 2-ME was between 0.78 μM and 200 μM. A549 cell viability was lowered after treatment with 100 μM 2-ME down to 76.26% and with 200 μM 2-ME down to 75.49% for 48 h (Fig. 1B).

Subsequently, analysis of the inhibitory activity of 2-ME against A549 cells was performed. We found that the compounds we had selected were capable of significantly reducing the viability of A549 cells. The inhibitory activity was estimated from IC50 values within the micromolar ranges. The IC50 value for 2-ME is dependent on the type of cell culture (Fig. 1C).

3.3. Induction of ROS signal in 2-ME-treated A549 cell culture

Consequently, we examined the level of intracellular oxidative stress in 2-ME-treated A549 cells. We specifically measured the level of hydrogen peroxide in 2-ME-treated A549 cells. A549 cells were treated with 2-ME at physiological (10 nM) and pharmacological (100 nM, 1 μM) concentrations according to the experimental design. The level of oxidative stress as measured by hydrogen peroxide concentration proved to be significantly higher in 2-ME treated A549 cell relative to the non-treated cells or the culture medium with no cell at all (Fig. 2A).

3.4. 2-ME-induced cell death (necrosis and late apoptosis) in lung cancer cellular model

Subsequently, the level of late apoptotic and necrotic cell death of 2-

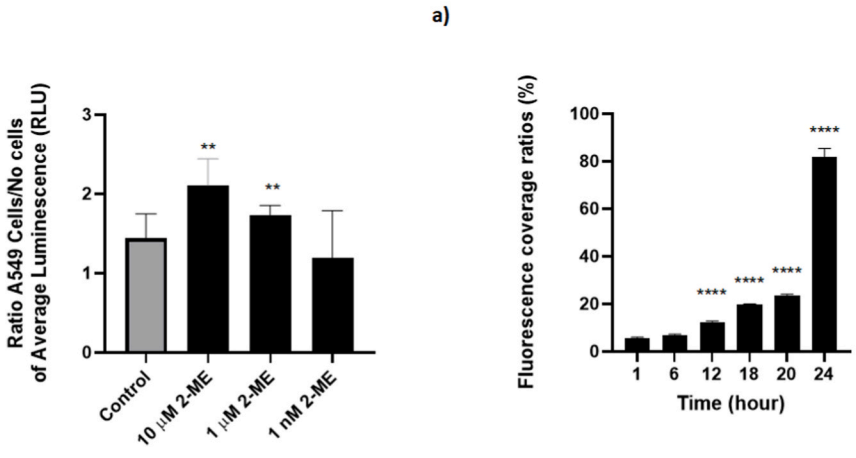

Fig. 2. (A) A549 cells as well as cell medium alone were treated with 2-ME at 10 μM, 1 μM and 10 nM concentrations, respectively. 2-ME treated A549 cells generated higher total hydrogen peroxide levels as compared to untreated control A549 cells incubated with Nutrient Mixture F-12 Ham medium alone. The obtained result comparing ROS induction in the wells with no cells and in the wells with A549 cells, indicates an increased production of ROS by the cancer cells. Luminescence was determined with a Glo-Max® Luminometer from Promega (Mannheim, Germany). Statistical analysis was performed using the GraphPad TTEST function (GraphPad Prism 9 version 9.0.0.). For analysis, both the mean of average luminescence (RLU) and the standard deviation were calculated. **(B)** Time-dependent growth rate of 2-ME-treated A549 cells. A549 cells treated with 2-ME 10 μM concentration up to 24 h. The analysis of the obtained results evaluated by staining with propidium iodide (PI) was performed using the CytoSMART Analysis System (Lux 3, CytoSMART, Eindhoven, The Netherlands). Values are presented as the mean ± SE of three independent experiments. *p < 0.01, **p < 0.001, ***p < 0.0001, ****p < 0.00001 vs. control cells.

ME-treated A549 cells was detected using propidium iodide (PI) labeling of technique. The A549 cells were treated with 2-ME at 10 μM concentration for 24 h. The increase in the fluorescence coverage factors was recorded 20 h after the start of the experiment at the fluorescence level to 23.25%. Related to cell confluence, the coverage target dropped to 22.90% after 24 h. Similarly, 24 h after the start of the 2-ME experiment, an increase in fluorescence to 85.17% was noted, which in our experiment was the highest level of cell death (Fig. 2B).

3.5. BAX-mediated 2-ME-induced cell death in lung cancer cellular model

Previously, we confirmed that the intrinsic pathway and BAX was activated by 2-ME in osteosarcoma 143B cells [2]. Herein, in order to further analyze the activation of BAX in 2-ME anticancer mechanism of action, we decided to use a BAX-inhibiting peptide, namely V5 [56]. It is as effective as the Caspase Inhibitor VI (Z-VAD-FMK; Cat. No. 219007) [2] for BAX-mediated apoptosis cellular model (~50–200 μM) [2]. Thus, the V5 inhibitor effectively blocks caspase-independent necrotic cell death [2].

Herein, the cells were pre-treated with 100 μM V5 peptide for 4 h, and then treated with 2-ME at a representative 1 μM concentration for 24 h. As demonstrated, pre-treatment with V5 reversed antiproliferative effect of 2-ME toward the lung cancer A549 cells (Fig. 3A).

3.6. S-palmitoylation as potential 2-ME mechanism of action in lung cancer cells

Based on our previous studies [2,6,25], we focused on a potential role of S-palmitoylation in BAX-mediated apoptosis. Palmostatin B (PalmB) being an APT1 inhibitor [57] was used in the study. Herein, the cells were treated with 100 μM PalmB and 2-ME at a representative 1 μM concentration, both separately and in combination, for 24 h. As demonstrated, treatment with either PalmB or 2-ME significantly decreased A549 cell viability (by ca. 30% as compared with control cells). Notably, we observed a synergistic effect on A549 cell viability of the two agents (PalmB and 2-ME) used in combination (Fig. 3B).

3.7. 2-ME as potent APT inhibitor

In order to investigate a potential impact of 2-ME on APT, we further performed molecular modeling studies. The two most representative structures of the binding complexes of 2-ME with APT1 and APT2, respectively, together with the RMSD plot and 2D pictures of the residues surrounding the ligand within the binding pocket, are shown in Fig. 4. Although the two APT proteins have a sequence similarity of 67%, the amino acid residues involved in the binding with 2-ME are different. This induces a remarkably different orientation of the ligand molecule inside the similar binding pocket. In detail, the bulky methyl group in position 13 of 2-ME, within APT1 and APT2 is oriented downward and

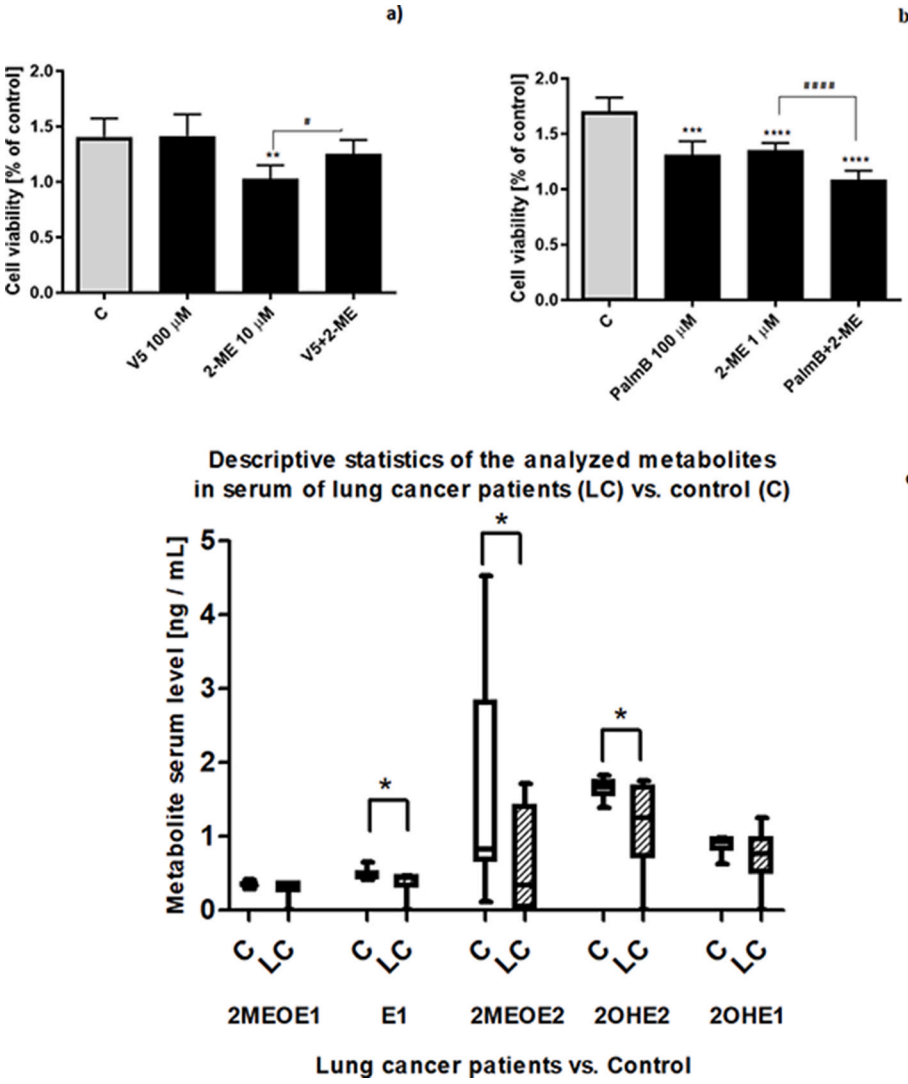

Fig. 3. (A). A549 cells were pretreated with V5 peptide at a concentration of 100 μM for 4 h, and then treated with 1 μM 2-ME for 24 h. Values are the mean ± SD of three independent experiments. *p < 0.01, **p < 0.001, ***p < 0.0001, ****p < 0.00001 vs. control cells. **(B)** The cells were treated for 24 h with either 100 μM PalmB or 10 μM 2-ME, and a combination of both. Both PalmB and 2-ME alone, significantly decreased A549 cell viability. A synergistic effect on the viability decrease was observed for treatment with both PalmB and 2-ME used in combination. The cell viability was determined by MTT assay. Values are presented as the mean ± SE of three independent experiments. *p < 0.01, **p < 0.001, ***p < 0.0001, ****p < 0.00001 vs. control cells C. Serum levels of critical estrogen metabolites analyzed in lung cancer patients (LC) as compared with healthy control (C) are presented as median, as well as quartile 1 and 3, with the minimum and maximum values, in the form of a typical box and whiskers plot. Statistically significant differences are marked with an asterisk * and refer to p-value < 0.05. It is worth noting that 2-ME serum level is significantly lower in lung cancer patients as compared with the control group. Based on table No 2.

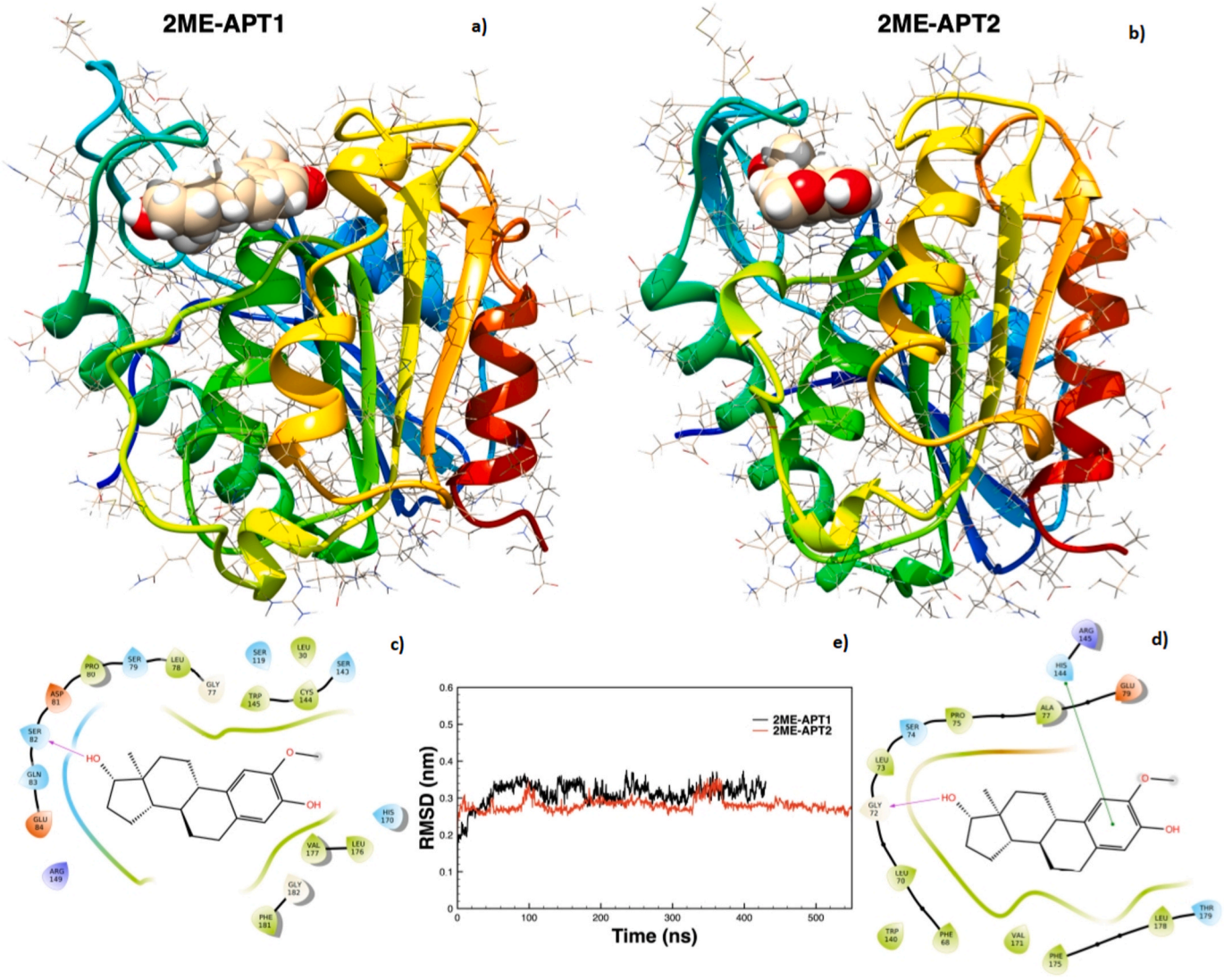

Fig. 4. The binding of 2-ME with APT1 **(A)** and APT2 **(B)** at the end of the MD trajectory. The two-dimensional protein residues surrounding the ligand **(C)**, **(D)**, and the RMSD plots are also shown (mean square displacement (RMSD) plots of the MD trajectory) **(E)**.

upward, respectively (Fig. 4). The different orientation is a compromise representation, which maximizes the stabilizing hydrophobic and H-bond interactions, and reduces the steric repulsions of the ligand with the protein backbone. As a result, 2-ME is able to enter more effectively inside the binding pocket of APT1, as compared to APT2 and the 2-ME molecule is in a more external position relative to the binding site of the APT2 protein. For the same reason, the binding pocket in APT1 results more enlarged upon binding with 2-ME, as compared to APT2. These considerations support the hypothesis that 2-ME binds more selectively to APT1 rather than APT2. The obtained results suggest that the selective binding of 2-ME to an APT1 protein molecule might indeed potentially enhance the anticancer effect of PalmB as was experimentally proven (see Results section 3.6).

3.8. Cancer progression and estrogen derivatives serum levels

In order to give our study a translational value, we next verified the serum levels of the studied estrogens in NSCLC patients. We specifically verified the levels of estrogens which are known to be used for physiological synthesis of 2-ME (2-MEOE2), namely estrone (E1), 17β-estradiol (E2), 2-hydroxyestradiol (2-OHE2), 2-hydroxyestrone (2OHE1) and 2-methoxyestrone (2-MEOE1). As determined by clinical analyses, we observed significantly decreased serum levels of 2-ME as compared with the control group (Table 2, Fig. 3C). A bunch of statistically significant differences were observed relative to critical estrogen metabolites, of which the lower serum concentrations of 2MEOE2 (2-ME) and 2OHE2 as detected in the lung cancer patients vs. control subjects are specifically noteworthy.

Similarly, much smaller decrease in estrogen metabolite levels in cancer patients as compared to the control group, could be noticed in the case of E1, 2MEOE1 and 2OHE1 (Fig. 3C). Interestingly, the parent molecule, namely E2, is only very slightly decreased in lung cancer patients as compared to control.

We thus hypothesize that hydroxylation at position 2 of the estradiol molecule, followed by methylation is a physiological anticancer protection mechanism. In order to better illustrate the biochemical relationships between different estrogen derivatives, we present the metabolic context involving natural estrogen biochemistry in the graphical form- Fig. 3C & graphical abstract.

3.9. Relative safety of 2-ME in terms of possible non-receptor bioactivity

The expected reactivity of 2-ME against weak nucleophiles of cytoprotective importance (glutathione, protein thiolates) as well as against

Table 2
Descriptive statistics of the analyzed metabolites in the group of lung cancer patients and the control. * Mann-Whitney *U* test; 1 - lung cancer patients, 2 - control group.

Variable	M		Me		SD		Min		Max		Q1		Q3		Statistical test result *
	1	2	1	2	1	2	1	2	1	2	1	2	1	2	
2MEOE1	0.28	0.34	0.35	0.34	0.15	0.03	0	0.29	0.36	0.42	0.26	0.34	0.36	0.35	**U = 39,5; p = 0,27; η2 = 0,06**
E1	0.36	0.49	0.44	0.48	0.19	0.07	0	0.41	0.47	0.65	0.33	0.44	0.45	0.5	**U = 20; p = 0,01; η2 = 0,29**
2MEOE2 (2-ME)	0.59	1.61	0.34	0.83	0.71	1.42	0	0.12	1.71	4.53	0.04	0.68	1.4	2.81	**U = 20; p = 0,047; η2 = 0,21**
2OHE2	1.11	1.63	1.25	1,67	0,64	0,13	0	1.39	1.75	1.83	0.73	1.57	1.66	1.74	**U = 23; p = 0,02; η2 = 0,24**
2OHE1	0.7	0.88	0.76	0.93	0.41	0.11	0	0.63	1.25	0.98	0.51	0.83	0.97	0.97	**U = 32; p = 0,29; η2 = 0,06**

amino groups of proteins and nucleic acids, estimated by calculation of its molecular electrophilic potential, was shown to be extremely low (electrophilic potential ω = 0.53 eV) as compared to the highly reactive electrophiles, and specifically the potentially mutagenic 2,3-estradiol-ortho-benzoquinone (ω = 3.59 eV) and its methine isomer (ω = 2.28 eV), or 3,4-ortho-benzoquinone of estradiol (ω = 3.63 eV). Thus, it can be assumed that the methoxy group of 2-ME is effective in preventing the spontaneous oxidation of catechol to highly reactive quinone derivatives of huge electrophilic potential, and consequently, against enzymatically uncontrolled, non-receptor-mediated damage to biomolecules essential for maintaining homeostasis at the cellular level, which makes 2-ME appear to be a relatively safe drug with a predictable and experimentally proven mechanism of action. The lipophilic nature of 2-ME (logP = 3.59) and the relatively small polar surface area of the molecule (PSA = 49.69 $Å^2$) ensure effective penetration through lipid bilayers and hence good bioavailability in different subcellular compartments and organelles of tumor cells. Interestingly, electrophilic potential of 2-ME parent molecules and biochemical conversion pathway intermediates, which were evaluated in clinical tests, also proved to be relatively low, as calculated for estradiol (ω = 0.66 eV), estrone (ω = 0.85 eV), 2-hydroxyestradiol (ω = 0.57 eV), and 2-hydroxyestrone (ω = 0.79 eV).

4. Discussion

Lung adenocarcinoma is one of the major non-small cell neoplasms of the lungs. Importantly, it is the most common lung cancer type in never-smoking patients. It should be emphasized that the incidence of this type of cancer in women is three times higher than in men. There is a possibility that 17β-estradiol metabolites may affect the death/survival interplay of lung adenocarcinoma cells by activating the nitroxidative stress signaling pathways or affecting metabolic regulatory mechanisms.

Epidemiological data show a significant increase in the incidence of malignant neoplasms, including lung cancer, among women [16]. The *p53* suppressor gene mutation in NSCLC was found to be significantly more frequent in women [59,60]. It is worth emphasizing the essence of female sex hormones, whose pro-carcinogenic and mitogenic effects are often of critical importance in clinical practice and scientific research. The correlation of oral contraceptives (OC) as well as hormone replacement therapy (HRT) with a significantly increased incidence of cancer has already been repeatedly described in the scientific literature [62,63]. There are two types of estrogen receptors ER: ERα and ERβ, the presence of which is necessary to maintain the proper condition of the extracellular matrix in the lung tissue [1]. Moreover, ERβ is present in both tissues and cell lines of NSCLC, which has been recognized as a prognostic marker so far [1].

Indeed, we have previously evidenced that the estrogenic activity of 2-ME at pharmacological concentration range is associated with the ERβ modulation [64].

Herein, we provide a new insight into anticancer mechanism of action of 2-ME in both 2D and 3D NSCLC cell models. Interestingly, many studies have investigated a high research potential of using 3D spheroidal lung cancer cell culture [65–67].

3D spheroidal cell cultures have a significant advantage over the commonly used 2D cell cultures. Both morphologically and physiologically, 3D cultures mimic the natural microenvironment of neoplastic cells in a much more natural and precise way, which allows for a better approximation of the *in vivo* conditions [68,69]. In response to unfavorable reports based on drug susceptibility studies in cultures of nodular lung cancer tumors, we similarly assessed the metabolites of 2-ME *in vitro*, with very promising results [70,71]. Based on the available literature data, in order to determine the anti-tumor potential of 2-ME, as well as due to the increased resistance of 3D cell cultures *in vitro*, which are similar in structure to neoplastic tumors *in vivo*, it was necessary to use a higher concentration of 2-ME. To the best of our knowledge, this is the first study to determine the effect of 2-ME on A549 cell death in a 3D model.

4.1. The mechanism of action of 2-ME depends on the induction of nitro-oxidative stress

Considering the nature of ROS in the tumor microenvironment, the essence of hypoxia should be particularly emphasized [72,73]. Importantly, the significance of hypoxia analogously to ROS impact within the tumor microenvironment should also be noted, as this phenomenon influences further metastasis from primary neoplastic tumors [49,62]. Moreover, it also influences angiogenesis process in the neoplastic tumor environment. HIF-1α inhibition may be one of the potential therapeutic options for treatment of malignant neoplastic tumors. Importantly, 2-ME displays an inhibitory effect on the HIF-1α protein [60,73].

Similarly to our studies on NSCLC cell models, according to the available data, sulfamoylated analogs of 2-ME, which influence the proliferation of MCF-7 and MDA-MB-231 breast cancer cells, were investigated in the study of the role of ROS in breast cancer [61]. These studies showed that sulfamoylated estradiol induced generation of superoxide anion and hydrogen peroxide. To the best of our knowledge, herein, for the first time we have indicated an increase in the oxidative stress level caused by 2-ME at selected reference concentrations in A549 cells, relative to untreated cells. As indicated by the available data, lung cancer cells, including the A549 cell line, react similarly to treatment with hydrogen peroxide as in our research, with cell cycle arrest at G1 phase, tumor necrosis, as well as apoptosis [74]. The study by Park et al. [74] clearly correlates with our observations evidently supporting our hypothesis. The obtained results are in correlation with available scientific data [75–79].

4.2. Association of palmitoylation mechanism with lung cancer cells

In order to investigate an anti-tumor role of 2-ME and further its more detailed mechanism of action, we decided to define the most important potential biological roles of the compound in lung adenocarcinoma, which would involve cytosolic enzymes, palmitoylation, reactive oxygen species generation, as well as the effect of the compound on induction of cell death. Cytosolic enzymes such as acyl-protein thioesterase 1 (APT1) and 2 acyl-protein thioesterase 2 (APT2), play an important role in different biological processes [80]. The role of APT1 and APT2 was also an object of our research based on specifically designed cell culture models. Protein S-palmitoylation is a covalent attachment of fatty acid acyl residue to the sulfhydryl group of a cysteine

moiety. In terms of carcinogenesis process, in particular, the zDHHC, PAT or APT enzymes, and more specifically APT1 and APT2, should be in particular taken into account [80]. According to the available data, it is more chemically effective to prevent the depalmitoylation process rather than to enhance protein palmitoylation [80]. Importantly, the inhibition of APT enzymes may inhibit the process of tumor formation, also having a toxic effect on tumor cells [80]. Hence, one of our goals was to investigate a potential anti-tumor activity mediated by APT modulation and consequently, via palmitoylation. APT1 and APT2 are expressed and active across nearly all tissues [81–83], yet their absence in most large-scale profiling research efforts suggests a non-stoichiometric relationship. Both APT1 and APT2 act as efficient depalmitoylases *in vitro* [84] and are presumed to broadly regulate S-palmitoylation and thus trafficking of some peripheral membrane proteins within the cell. Furthermore, overexpression of APT1 enhances the depalmitoylation of small GTPases interacting with endothelial nitric oxide synthase [85], and a number of other peripheral membrane proteins in transfected cells. Such overexpression could lead to a number of potential artifacts, e.g. by disruptive fusion. Consistently with these studies, our results strongly support the hypothesis of 2-ME binding selectively to APT1 rather than APT2. From a biochemical point of view, APT2 is functionally closely related to palmitoylation of protein substrates [86].

As indicated by the available studies in the field of neurodegenerative diseases [86], oxidative stress is often involved in the range of lipid signaling modulation, including palmitoylation, which is actually the subject of our research. The oxidative stress mechanism has been shown to directly inhibit palmitoylation by disrupting lipid mediator signaling and causing destructive effects on the cellular metabolism [87]. Hence, after having examined the effects of H2O2 on lung cancer cells, we decided to determine a potential role of S-palmitoylation in BAX-mediated apoptosis of A549 cells.

An equally significant aspect of our research is the investigation of a depalmitoylation inhibitor, namely PalmB. Unfortunately, the literature data on a potential effect of PalmB on NSCLC is very limited. Our critical achievement is an unambiguous proof of the synergistic effect of PalmB and 2-ME used in combination on a significant A549 cell viability reduction. Furthermore, based on the previous research [17], and also on the results obtained from our study, we hypothesize that 2-ME influences an increase in S-palmitoylation in the A549 cells, which seems to positively correlate with an observed increase in apoptosis-dependent cell death possibly via BAX protein palmitoylation.

4.3. A unique estrogen derivatives profile in the plasma from NSCLC patients potentially relating to lung cancer etiopathogenesis and progression

Based on our research, we conclude that targeting estrogen levels in lung cancer patients is a promising diagnostic, monitoring and therapeutic approach. In recent years, there has been much improvement in lung cancer treatment, including NSCLC, however, for most patients, lung cancer is a fatal disease, which is mainly caused by delayed diagnosis of very advanced cancer stage [29].

Current scientific reports [88–90] indicate a correlation between the endocrine system, mainly in women, and the increase in lung cancer incidence, especially NSCLC. Therefore, based on the finding of such relationship and the involvement of estrogen signaling in lung adenocarcinoma, combination therapies based on antiestrogen therapy and tyrosine kinase inhibitors (TKI) were assessed [88]. Moreover, available bioinformatics analyses indicate that ERs can directly influence modulation of NSCLC molecular pathways, primarily through signal transduction, as well as an activation of membrane receptors, which ultimately changes the morphology of NSCLC cells [89]. E2, showing immunosuppressive properties, directly influences the pro-cancer microenvironment [90]. Moreover, analogously to lung cancer, E2 has been shown to directly affect lung stromal cells as well as lung immune cells [90]. One of the studies was devoted to the assessment of estrogens and their metabolites in the lung tissue of women suffering from lung cancer, and in the control group [91].

On the basis of the obtained results, it was possible to establish that estrogens, and specifically E1, E2, E3, and their metabolites: 2-OHE1, 2-OHE2, 4-OHE1, 4-OHE2, 2-OME1 and 2-OME2, are found at much higher levels in the lung neoplastic tissue than in the lung tissue of healthy female control [91]. These results indicate that estrogens and their metabolites are found in the tissues of the human lung at substantial levels [91]. Moreover, the determination of estrogen metabolite levels, either in blood or urine samples obtained from clinical patients, may be used as a replacement biomarker for breast cancer risk [92]. As we observed in the performed clinical tests, the level of 2-ME significantly drops in lung cancer patients, which can be utilized for screening diagnostic tests as well as for monitoring progression of the disease in the course of anticancer therapy. Hence, our hypothesis is to a large extent based on the determination of the observable effects of estrogens and their metabolites found in the blood of lung cancer patients on cancer incidence and progression.

In summary, the results of our study indicate for the first time to the best of our knowledge, a possible use of estrogens both hydroxylated and methylated at position 2, as NSLC tumor biomarkers. Obviously, more complex clinical studies including larger patient groups are necessary.

Our results open up an exciting new research pathways focusing on more advanced and comprehensive clinical trials with routine application of blood tests in order to better monitor lung cancer patients and healthy controls, as well as developing sophisticated *in vitro* experiments with other lung cancer cell lines, specifically in 3D cell culture model. Nevertheless, the obtained results seem to be potentially applicable in the process of clinical diagnosis and monitoring of NSCLC patients in the near future.

4.4. Safety profile of 2-ME as a potential therapeutic in terms of non-receptor mediated biological activity

We managed to prove beyond doubt on A549 cancer cell models that 2-ME has a strong anti-tumor activity. It might be potentially applied as a therapeutic in the form of an adjuvant or neoadjuvant in the course of lung cancer treatment. However, many estrogen metabolites are suspected of potentially deleterious non-receptor-mediated biological effects that could damage noncancer cells in the body giving rise to serious clinical complications. Computational analysis of 2-ME electrophilic potential proved that it is relatively low as compared to catechol estrogen quinones which are known to be highly reactive with nucleophiles of biological importance, and consequently deplete cellular glutathione level and covalently modify DNA causing generation of severe oxidative stress, and ultimately carcinogenesis [93,94]. The electrophilic potential of 2-ME ($\omega = 0.53$ eV) being less than 0.8 eV, classifies 2-ME as a marginal electrophile according to the electrophilicity scale as proposed by Domingo et al. [95]. Catechol estrogen quinones, such as 2,3-estradiol-ortho-benzoquinone ($\omega = 3.59$ eV) and its methine isomer ($\omega = 2.28$ eV), or 3,4-ortho-benzoquinone of estradiol ($\omega = 3.63$ eV) are quite the contrary, classified as very strong electrophiles as their potential is much greater than 1.5 eV [95]. Thus they are expected to readily create conjugates with glutathione, protein thiols as well as adducts with the DNA. Catechol estrogen quinones conjugation with biologically critical thiols is based on the Michael addition reaction mechanism which is not enzymatically controlled. Taking into account relatively high millimolar levels of cellular glutathione, hence estrogen quinones are rate limiting reactants for the process which makes them specifically dangerous in terms of potential carcinogenesis.

A physiological protection mechanism preventing the excess formation of estrogen quinones is based on O-methylation of catechol estrogens at position 2 or 4 by catechol O-methyltransferase (COMT) into methoxylated estrogens such as 2-methoxyestradiol, 2-methoxyestrone, 4-methoxyestradiol and 4-methoxyestrone which are all either very

weak or marginal electrophiles. As we demonstrated in NSCLC patients, the serum levels of 2-ME are significantly lower than in healthy control with a simultaneously slightly lower level of its parent catechol molecule, 2-hydroxyestradiol (2OHE2). It may suggest that in the group of lung cancer patients there is an impaired O-methylation of catechols which consequently fuel an alternative metabolic pathway catalyzed by cytochrome P450 and peroxidases as well as through non-enzymatic, oxidative stress-mediated mechanisms, into potentially carcinogenic catechol estrogen quinones [93,94].

That is why, determination of 2-ME level in patient's blood or urine might be utilized as a reasonable screening test allowing for lung cancer early diagnosis and prevention as well as a convenient way to monitor progression of the disease. The idea of using 2-ME as an anti-cancer drug of well defined mechanism of action, and at the same time, a relatively safe one due to its low electrophilic potential, for effective adjuvant or neoadjuvant therapy of NSCLC, seems very tempting, however, it definitely demands further research and specialized clinical trials.

5. Conclusions

Herein, we presented a complex research study, regarding further investigation of 2-ME anti-tumor detailed mechanism of action. Using an experimental non-small-cell lung carcinoma model, it was shown that 2-ME inhibited tumor cell viability, both in a commonly used *in-vitro* two-dimensional model as well as in 3D spheroidal cellular models. In addition, it was determined that ROS generation was increased in A549 cells as a result of 2-ME treatment. The presence of necrotic/late apoptotic cells following treatment with 2-ME was also confirmed via green and red fluorescence. Moreover, has been proven that 2-ME significantly decreases A549 cell viability as compared to combination treatment with 2-ME and V5. Very importantly, the study showed a synergistic inhibitory effect of 2-ME and PalmB used in combination on lung cancer call viability. Only APT1 is located primarily in the mitochondria. This indicates that this may be a new spectrum for APT1 only substrates, where they are unavailable for APT2. Hence, it opens up a new area of research in the field of 2-ME and APT1 and APT2 relative to cell death [96]. The evidence from the study implied that 2-ME might serve as a prognostic and monitoring biomarker in lung cancer patients. Moreover, the results of our research on A549 lung adenocarcinoma cells suggested that 2-ME should work as an effective APT inhibitor increasing the level of cellular protein palmitoylation. We also hypothesized that 2-ME effect on palmitoylation might be clinically applicable as a novel target for anti-cancer therapy. The review of scientific publications on the issues raised by our team so far indicates that the right direction of research has been chosen [97–104].

Moreover, computational analysis proves that 2-ME as compared to other estrogen metabolism intermediates is relatively safe in terms of its possible non-receptor bioactivity within healthy human cells due to a very low electrophilic potential and hence no substantial risk of spontaneous covalent modification of biologically protective nucleophiles. Lipophilic character of 2-ME suggests effective penetration through lipid membranes and optimal interaction with hydrophobic domains of critical proteins within cancer cells.

It is worth mentioning that clinical application of the conclusions from our study would not cause much of a problem as it mostly involves determination of specific estrogen metabolites in patients' blood or even better in urine which makes it a practically non-invasive diagnostic approach which in addition to that, is relatively fast and affordable.

All in all, the developed methodology has found its practical dimension, and moreover, strongly supports the anti-tumor activity of 2-ME and its potential role in clinical diagnosis, monitoring and potential anticancer therapy.

Funding

The study was funded by IDUB Program's Research Project for Young Scientist MTN No 71–1203 (Medical University of Gdansk, Gdansk, Poland).

MGP & NK acknowledge support from ST46 funding (Medical University of Gdansk, Gdansk, Poland) for molecular modeling computation system.

Data availability

The data used to support the findings of this study are available from the corresponding author upon request.

Declaration of competing interest

The authors declare no conflict of interest.

Acknowledgments

MGP, AKJ & NK acknowledge support from ST46 funding (Medical University of Gdansk, Gdansk, Poland). This research was supported in part by PLGrid Infrastructure providing Gaussian 09 chemical computational software (revision D.01 by Frisch, M. J. et al., [2016]) as well as GaussView v.5.0.8. (NK).

Marvin ChemAxon Academic License was used for drawing, displaying and characterizing chemical structures, Marvin 20.21, ChemAxon (https://www.chemaxon.com). (NK) Multifunctional Wavefunction Analyzer (Multiwfn, v. 3.3.8 by Tian Lu, Feiwu Chen, J. Comp. Chem. 33, 580–592 [2012]).

We would like to thank dr Michal Ordak (Ekspertat) for his assistance in statistical analysis.

We would like to thank CytoSMART (CytoSMART, Eindhoven, The Netherlands), for providing the CytoSMART Omni automated bright-field microscope, CytoSMART Lux2 compact automated system and the Cytosmart LUX3 imaging system consisting of two fluorescence microscopes devices to our research project, as well as the Promega manufacturer (Mannheim, Germany), for providing the GloMax® Discover Microplate Reader, which enriched the value of our research.

Appendix A. Supplementary data

Supplementary data to this article can be found online at https://doi.org/10.1016/j.redox.2022.102395.

References

[1] C. Musial, R. Zaucha, A. Kuban-Jankowska, L. Konieczna, M. Belka, A. Marino Gammazza, T. Baczek, F. Cappello, M. Wozniak, M. Gorska-Ponikowska, Plausible role of estrogens in pathogenesis, progression and therapy of lung cancer, Int. J. Environ. Res. Publ. Health 18 (2) (2021) 648.

[2] M. Gorska-Ponikowska, P. Bastian, A. Zauszkiewicz-Pawlak, et al., Regulation of mitochondrial dynamics in 2-methoxyestradiol-mediated osteosarcoma cell death, Sci. Rep. 11 (2021) 1616.

[3] M.H. Kulke, J.A. Chan, J.A. Meyerhardt, A.X. Zhu, T.A. Abrams, L. S. Blaszkowsky, E. Regan, C. Sidor, C.S. Fuchs, A prospective phase II study of 2-methoxyestradiol administered in combination with bevacizumab in patients with metastatic carcinoid tumors, Cancer Chemother. Pharmacol. 68 (2) (2011) 293–300.

[4] J.Y. Bruce, J. Eickhoff, R. Pili, T. Logan, M. Carducci, J. Arnott, A. Treston, G. Wilding, G. Liu, A phase II study of 2-methoxyestradiol nanocrystal colloidal dispersion alone and in combination with sunitinib malate in patients with metastatic renal cell carcinoma progressing on sunitinib malate, Invest. N. Drugs 30 (2) (2012) 794–802.

[5] M. Gorska-Ponikowska, A. Ploska, D. Jacewicz, M. Szkatula, G. Barone, G. Lo Bosco, F. Lo Celso, A.M. Dabrowska, A. Kuban-Jankowska, M. Gorzynik-Debicka, N. Knap, L. Chmurzynski, L.W. Dobrucki, L. Kalinowski, M. Wozniak, Modification of DNA structure by reactive nitrogen species as a result of 2-methoxyestradiol-induced neuronal nitric oxide synthase uncoupling in metastatic osteosarcoma cells, Redox Biol. 32 (2020), 101522.

[6] M. Gorska-Ponikowska, A. Kuban-Jankowska, A. Daca, S. Nussberger, 2-Methoxyestradiol reverses the pro-carcinogenic effect of L-lactate in osteosarcoma 143B cells, Cancer Genomics Proteomics 14 (2017) 483–493.

[7] M. Gorska-Ponikowska, A. Kuban-Jankowska, S.A. Eisler, U. Perricone, G. Lo Bosco, G. Barone, S. Nussberger, 2-Methoxyestradiol affects mitochondrial

biogenesis pathway and succinate dehydrogenase complex flavoprotein subunit A in osteosarcoma cancer cells, Cancer Genomics Proteomics 15 (1) (2018) 73–89.
[8] M. Gorska, A. Kuban-Jankowska, R. Milczarek, M. Wozniak, Nitro-oxidative stress is involved in anticancer activity of 17β-estradiol derivative in neuroblastoma cells, Anticancer Res. 36 (4) (2016) 1693–1698.
[9] 2-Methoxyestradiol in Treating Patients with Advanced Solid Tumors, 2021. Available online, https://clinicaltrials.gov/ct2/show/NCT00028821?cond=panzem&draw=2&rank=8 (20/08/2021).
[10] A Combination Study to Determine the Safety and Efficacy of Panzem NCD with Avastin in Metastatic Carcinoid Tumors, 2021. Available online, https://clinicaltrials.gov/ct2/show/NCT00328497?cond=panzem&draw=2&rank=4 (20/08/2021).
[11] A Phase 2 Study with Panzem in Patients with Relapsed or Plateau Phase Multiple Myeloma, 2021. Available online, https://clinicaltrials.gov/ct2/show/NCT00592579?cond=panzem&draw=2&rank=6 (20/08/2021).
[12] A Combination Study to Determine the Safety and Efficacy of Panzem NCD with Avastin in Metastatic Carcinoid Tumors, 2021. Available online, https://clinicaltrials.gov/ct2/show/NCT00328497?term=panzem&draw=2&rank=2 (20/08/2021).
[13] Efficacy and Pharmacodynamic Study of Panzem® NCD in Patients with Hormone-Refractory Prostate Cancer, 2021. Available online, https://clinicaltrials.gov/ct2/show/NCT00394810?term=panzem&draw=2&rank=6 (20/08/2021).
[14] Phase 2 Study of Panzem Nanocrystal Colloidal Dispersion (NCD) in Combination With Fixed-Dose Temozolomide to Patients With Recurrent Glioblastoma Multiforme (GBM), 2021. Available online, https://clinicaltrials.gov/ct2/show/NCT00481455?term=panzem&draw=2&rank=5.
[15] M.R. Harrison, N.M. Hahn, R. Pili, W.K. Oh, H. Hammers, C. Sweeney, G. Liu, A phase II study of 2-methoxyestradiol (2ME2) NanoCrystalA (R) dispersion (NCD) in patients with taxane- refractory, metastatic castrate-resistant prostate cancer (CRPC), Invest. N. Drugs 29 (2011) 1465–1474.
[16] M.H. Kulke, J.A. Chan, J.A. Meyerhardt, A.X. Zhu, T.A. Abrams, L.S. Blaszkowsky, C.S. Fuchs, A prospective phase II studyof 2-methoxyestradiol administered in combination with bevacizumabin patients with metastatic carcinoid tumors, Cancer Chemother. Pharmacol. 68 (2011) 293–300.
[17] D. Matei, J. Schilder, G. Sutton, S. Perkins, T. Breen, C. Quon, C. Sidor, Activity of 2 methoxyestradiol (Panzem (R) NCD) inadvanced, platinum-resistant ovarian cancer and primary peritonealcarcinomatosis: a Hoosier Oncology Group trial, Gynecol. Oncol. 115 (2009) 90–96.
[18] E.J. Solum, Ø.W. Akselsen, A. Vik, T.V. Hansen, Synthesis and pharmacological effects of the anti-cancer agent 2-methoxyestradiol, Curr. Pharmaceut. Des. 21 (38) (2015) 5453–5466.
[19] B.S. Kumar, D.S. Raghuvanshi, M. Hasanain, S. Alam, J. Sarkar, K. Mitra, F. Khan, A.S. Negi, Recent Advances in chemistry and pharmacology of 2-methoxyestradiol: an anticancer investigational drug, Steroids 110 (2016 Jun) 9–34.
[20] P. Bastian, J. Dulski, A. Roszmann, D. Jacewicz, A. Kuban-Jankowska, J. Slawek, M. Wozniak, M. Gorska-Ponikowska, Regulation of mitochondrial dynamics in Parkinson's disease-is 2-methoxyestradiol a missing piece? Antioxidants 10 (2) (2021) 248.
[21] M. Gorska, A. Kuban-Jankowska, M.A. Zmijewski, M. Gorzynik, M. Szkatula, M. Wozniak, Neuronal nitric oxide synthase induction in the antitumorigenic and neurotoxic effects of 2-methoxyestradiol, Molecules 19 (2014) 13267–13281.
[22] M.E. Zaballa, F.G. van der Goot, The molecular era of protein S-acylation: spotlight on structure, mechanisms, and dynamics, Crit. Rev. Biochem. Mol. Biol. 53 (4) (2018) 420–451.
[23] P.J. Ko, S.J. Dixon, Protein palmitoylation and cancer, EMBO Rep. 19 (10) (2018), e46666.
[24] L. Abrami, M. Audagnotto, S. Ho, Palmitoylated acyl protein thioesterase APT2 deforms membranes to extract substrate acyl chains, Nat. Chem. Biol. 17 (2021) 438–447.
[25] M. Fröhlich, B. Dejanovic, H. Kashkar, G. Schwarz, S. Nussberger, S-palmitoylation represents a novel mechanism regulating the mitochondrial targeting of BAX and initiation of apoptosis, Cell Death Dis. 5 (2) (2014) e1057.
[26] C.S. Dela Cruz, L.T. Tanoue, R.A. Matthay, Lung cancer: epidemiology, etiology, and prevention, Clin. Chest Med. 32 (2011) 605–644.
[27] Z. Zhu, Z. Zheng, J. Liu, Comparison of COVID-19 and lung cancer via reactive oxygen species signaling, Front. Oncol. 11 (2021), 708263.
[28] J. Stepniak, M. Karbownik-Lewinska, 17β-estradiol prevents experimentally-induced oxidative damage to membrane lipids and nuclear DNA in porcine ovary, Syst. Biol. Reprod. Med. 62 (1) (2016) 17–21.
[29] D.J. Heineman, J.M. Daniels, W.H. Schreurs, Clinical staging of NSCLC: current evidence and implications for adjuvant chemotherapy, Ther Adv Med Oncol 9 (9) (2017) 599–609.
[30] L. Helguero, M. Faulds, J.Å. Gustafsson, Estrogen receptors alfa (ERα) and beta (ERβ) differentially regulate proliferation and apoptosis of the normal murine mammary epithelial cell line HC11, Oncogene 24 (2005) 6605–6616.
[31] W.D. Travis, E. Brambilla, A.P. Burke, A. Marx, A.G. Nicholson, WHO Classification of Tumours of the Lung, Pleura, Thymus and Heart, International Agency for Research on Cancer, Lyon, France, 2015.
[32] M. Gorska-Ponikowska, A. Ploska, D. Jacewicz, M. Szkatula, G. Barone, G. Lo Bosco, F. Lo Celso, A.M. Dabrowska, A. Kuban-Jankowska, M. Gorzynik-Debicka, N. Knap, L. Chmurzynski, L.W. Dobrucki, L. Kalinowski, M. Wozniak, Modification of DNA structure by reactive nitrogen species as a result of 2-methoxyestradiol-induced neuronal nitric oxide synthase uncoupling in metastatic osteosarcoma cells, Redox Biol. 32 (2020 May), 101522.
[33] M. Gorska-Ponikowska, P. Bastian, A. Zauszkiewicz-Pawlak, et al., Regulation of mitochondrial dynamics in 2-methoxyestradiol-mediated osteosarcoma cell death, Sci. Rep. 11 (2021) 1616.
[34] M. Gorska-Ponikowska, A. Kuban-Jankowska, A. Marino Gammazza, A. Daca, J. M. Wierzbicka, M.A. Zmijewski, H.H. Luu, M. Wozniak, F. Cappello, The major heat shock proteins, Hsp70 and Hsp90, in 2-methoxyestradiol-mediated osteosarcoma cell death model, Int. J. Mol. Sci. 21 (2020) 616.
[35] A. Sali, T.L. Blundell, Comparative protein modelling by satisfaction of spatial restraints, J. Mol. Biol. 234 (3) (1993) 779–815.
[36] A. Fiser, A. Šali, MODELLER: generation and refinement of homology-based protein structure models, in: C.W. Carter, R.M. Sweet (Eds.), Methods in Enzymology, vol. 374, Academic Press, San Diego, 2003, pp. 463–493.
[37] O. Trott, A.J. Olson, AutoDock Vina: improving the speed and accuracy of docking with a new scoring function, efficient optimization, and multithreading, J. Comput. Chem. 31 (2) (2010) 455–461.
[38] A. Kuban-Jankowska, T. Kostrzewa, C. Musial, G. Barone, G. Lo Bosco, F. Lo Celso, M. Gorska-Ponikowska, Green tea catechins induce inhibition of PTP1B phosphatase in breast cancer cells with potent anti-cancer properties: in vitro assay, molecular docking, and dynamics studies, Antioxidants 9 (12) (2020) 1208.
[39] M. Gorska-Ponikowska, U. Perricone, A. Kuban-Jankowska, G. Lo Bosco, G. Barone, 2-methoxyestradiol impacts on amino acids-mediated metabolic reprogramming in osteosarcoma cells by its interaction with NMDA receptor, J. Cell. Physiol. 232 (2017) 3030–3049.
[40] K. Lindorff-Larsen, S. Piana, K. Palmo, P. Maragakis, J.L. Klepeis, R.O. Dror, D. E. Shaw, Improved side-chain torsion potentials for the Amber ff99SB protein force field, Proteins 78 (8) (2010) 1950–1958.
[41] E. Lindahl, B. Hess, D. van der Spoel, Gromacs 3.0: a package for molecular simulation and trajectory analysis, J. Mol. Model. 7 (2001) 306–317.
[42] V. Zoete, M.A. Cuendet, A. Grosdidier, O. SwissParam Michielin, A fast force field generation tool for small organic molecules, J. Comput. Chem. 32 (2011) 2359–2368.
[43] G. Bussi, D. Donadio, M. Parrinello, Canonical sampling through velocity rescaling, J. Chem. Phys. 126 (1) (2017), 014101.
[44] M. Parrinello, Polymorphic transitions in single crystals: a new molecular dynamics method, J. Appl. Phys. 52 (1981) 7182–7190.
[45] T. Darden, Particle mesh Ewald: an N·log(N) method for Ewald sums in large systems, J. Chem. Phys. 98 (1993) 10089–10092.
[46] U. Essmann, L. Perera, M.L. Berkowitz, A smooth particle mesh Ewald method, J. Chem. Phys. 103 (1995), 8577-8493.
[47] F. Camastra, R. Amato, M.D. Di Taranto, A. Staiano, Advances in computational methods for genetic diseases, Comput. Math. Methods Med. 645649 (2015).
[48] R. Giancarlo, F. Utro, Speeding up the Consensus Clustering methodology for microarray data analysis, Algorithm Mol. Biol. 6 (2011) 1.
[49] R. Giancarlo, G.L. Bosco, L. Pinello, F. Utro, The three steps of clustering in the post-genomic era: a synopsis, in: R. Rizzo, P.J.G. Lisboa (Eds.), Computational Intelligence Methods for Bioinformatics and Biostatistics. CIBB 2010, Lecture Notes in Computer Science, vol. 6685, Springer, Berlin, Heidelberg, 2011.
[50] P. Söderhjelm, G.A. Tribello, M. Parrinello, Locating binding poses in protein-ligand systems using reconnaissance metadynamics, Proc. Natl. Acad. Sci. U. S. A. 109 (14) (2012) 5170–5175.
[51] S. Salentin, S. Schreiber, V.J. Haupt, M.F. Adasme, M. Schroeder, PLIP: fully automated protein-ligand interaction profiler, Nucleic Acids Res. 43 (W1) (2015) W443–W447.
[52] E.F. Pettersen, T.D. Goddard, C.C. Huang, G.S. Couch, D.M. Greenblatt, E. C. Meng, T.E. Ferrin, UCSF chimera—a visualization system for exploratory research and analysis, J. Comput. Chem. 25 (2004) 1605–1612.
[53] T. Koopmans, Über die Zuordnung von Wellenfunktionen und Eigenwerten zu den Einzelnen Elektronen Eines Atoms, Physica 1 (1933) 104–113.
[54] W. Kohn, L.J. Sham, Self-consistent equations including exchange and correlation effects, Phys. Rev. B 140 (1965) A1133–A1138.
[55] R.G. Parr, W. Yang, Density-functional theory of the electronic structure of molecules, Annu. Rev. Phys. Chem. 46 (1995) 701–728.
[56] R. Fernandes, C. Tsuda, A.L. Perumalsamy, et al., NLRP5 mediates mitochondrial function in mouse oocytes and embryos, Biol. Reprod. 86 (5) (2012), 138-10.
[57] F.J. Dekker, C. Hedberg, Small molecule inhibition of protein depalmitoylation as a new approach towards downregulation of oncogenic Ras signalling, Bioorg. Med. Chem. 19 (4) (2011) 1376–1380.
[58] T.M. LaVallee, X.H. Zhan, C.J. Herbstritt, E.C. Kough, S.J. Green, V.S. Pribluda, 2-Methoxyestradiol inhibits proliferation and induces apoptosis independently of estrogen receptors alpha and beta, Cancer Res. 62 (13) (2002) 3691–3697.
[59] G. Shen, Q. Wang, Q. Zhang, H. Sun, Y. Zhao, Z. Zhang, B. Du, Tissue distribution of 2-methoxyestradiol nanosuspension in rats and its antitumor activity in C57BL/6 mice bearing lewis lung carcinoma, Drug Deliv. 19 (7) (2012) 327–333.
[60] A. Aquino-Gálvez, G. González-Ávila, J. Delgado-Tello, M. Castillejos-López, C. Mendoza-Milla, J. Zúñiga, M. Checa, H.A. Maldonado-Martínez, A. Trinidad-López, J. Cisneros, L.M. Torres-Espíndola, C. Hernández-Jiménez, B. Sommer, C. Cabello-Gutiérrez, L.H. Gutiérrez-González, Effects of 2-methoxyestradiol on apoptosis and HIF-1α and HIF-2α expression in lung cancer cells under normoxia and hypoxia, Oncol. Rep. 35 (1) (2016) 577–583.
[61] Y. Romero, M. Castillejos-López, S. Romero-García, A.S. Aguayo, I. Herrera, M. O. Garcia-Martin, L.M. Torres-Espíndola, M.C. Negrete-García, A.C. Olvera, J. C. Huerta-Cruz, R.V. Cruz, J. Cisneros, E.F. Soto, H. Solís-Chagoyán, C. Mendoza-Milla, C. Cabello-Gutiérrez, V. Ruiz, A. Aquino-Gálvez, Antitumor therapy under hypoxic microenvironment by the combination of 2-methoxyestradiol and

sodium dichloroacetate on human non-small-cell lung cancer, Oxid. Med. Cell. Longev. (2020), 3176375.
[62] P.C. Rath, T. Mukhopadhyay, p53 gene expression and 2-methoxyestradiol treatment differentially induce nuclear factor kappa B activation in human lung cancer cells with different p53 phenotypes, DNA Cell Biol. 28 (12) (2009) 615–623.
[63] Y. Zhang, C.Y. Han, F.G. Duan, p53 sensitizes chemoresistant non-small cell lung cancer via elevation of reactive oxygen species and suppression of EGFR/PI3K/AKT signaling, Cancer Cell Int. 19 (2019) 188.
[64] T.E. Sutherland, M. Schuliga, T. Harris, B.L. Eckhardt, R.L. Anderson, L. Quan, A. G. Stewart, 2-methoxyestradiol is an estrogen receptor agonist that supports tumor growth in murine xenograft models of breast cancer, Clin. Cancer Res. 11 (5) (2005) 1722–1732.
[65] A. Mogi, H. Kuwano, TP53 mutations in nonsmall cell lung cancer, J. Biomed. Biotechnol. (2011), 583929.
[66] F. Saleh, A. Harb, N. Soudani, H. Zaraket, A three-dimensional A549 cell culture model to study respiratory syncytial virus infections, J Infect Public Health 13 (8) (2020) 1142–1147.
[67] H. Eguchi, R. Akizuki, R. Maruhashi, M. Tsukimoto, T. Furuta, T. Matsunaga, S. Endo, A. Ikari, Increase in resistance to anticancer drugs involves occludin in spheroid culture model of lung adenocarcinoma A549 cells, Sci. Rep. 8 (1) (2018), 15157.
[68] H. Eguchi, H. Matsunaga, S. Onuma, Y. Yoshino, T. Matsunaga, A. Ikari, Down-regulation of claudin-2 expression by cyanidin-3-glucoside enhances sensitivity to anticancer drugs in the spheroid of human lung adenocarcinoma A549 cells, Int. J. Mol. Sci. 22 (2) (2021) 499.
[69] F. Sambale, A. Lavrentieva, F. Stahl, C. Blume, M. Stiesch, C. Kasper, D. Bahnemann, T. Scheper, Three dimensional spheroid cell culture for nanoparticle safety testing, J. Biotechnol. 205 (2015) 120–129.
[70] S. Sant, P.A. Johnston, The production of 3D tumor spheroids for cancer drug discovery, Drug Discov. Today Technol. 23 (2017) 27–36.
[71] R. Di Liello, V. Ciaramella, G. Barra, M. Venditti, C.M. Della Corte, F. Papaccio, F. Sparano, G. Viscardi, M.L. Iacovino, S. Minucci, M. Fasano, F. Ciardiello, F. Morgillo, Ex vivo lung cancer spheroids resemble treatment response of a patient with NSCLC to chemotherapy and immunotherapy: case report and translational study, ESMO Open 4 (4) (2019), e000536.
[72] Y. Jo, N. Choi, K. Kim, H.J. Koo, J. Choi, H.N. Kim, Chemoresistance of cancer cells: requirements of tumor microenvironment-mimicking in vitro models in anti-cancer drug development, Theranostics 8 (19) (2018) 5259–5275.
[73] Y. Romero, A. Aquino-Gálvez, Hypoxia in cancer and fibrosis: Part of the problem and part of the solution, Int. J. Mol. Sci. 22 (15) (2021) 8335.
[74] W.H. Park, Hydrogen peroxide inhibits the growth of lung cancer cells via the induction of cell death and G1 phase arrest, Oncol. Rep. 40 (3) (2018 Sep) 1787–1794.
[75] H. Sherman, H.J. Gitschier, A.E. Rossi, A novel three-dimensional immune Oncology model for high-throughput testing of tumoricidal activity, Front. Immunol. 9 (2018) 857.
[76] M. Gorska, A. Kuban-Jankowska, M. Zmijewski, A. Marino Gammazza, F. Cappello, M. Wnuk, M. Gorzynik, I. Rzeszutek, A. Daca, A. Lewinska, M. Wozniak, DNA strand breaks induced by nuclear hijacking of neuronal NOS as an anti-cancer effect of 2-methoxyestradiol, Oncotarget 6 (17) (2015) 15449–15463.
[77] A. Parada-Bustamante, C. Valencia, P. Reuquen, P. Diaz, R. Rincion-Rodriguez, P. A. Orihuela, Role of 2-methoxyestradiol, an endogenous estrogen metabolite, in health and disease, Mini Rev. Med. Chem. 15 (5) (2015) 427–438.
[78] Górska Magdalena, Żmijewski Michał, Kuban-Jankowska Alicja, Wnuk Maciej, Rzeszutek Iwona, Woźniak Michał, Neuronal nitric oxide synthase-mediated genotoxicity of 2-methoxyestradiol in hippocampal HT22 cell line, Mol. Neurobiol. 53 (7) (2016) 5030–5040.
[79] Górska Magdalena, Wyszkowska Roksana Maja, Kuban-Jankowska Alicja, Woźniak Michał, Impact of apparent antagonism of estrogen receptor β by fulvestrant on anticancer activity of 2-methoxyestradiol, Anticancer Res. 36 (5) (2016) 2217–2226.
[80] A.J. Lee, M.X. Cai, P.E. Thomas, A.H. Conney, B.T. Zhu, Characterization of the oxidative metabolites of 17beta-estradiol and estrone formed by 15 selectively expressed human cytochrome p450 isoforms, Endocrinology 144 (8) (2003) 3382–3398.
[81] P.J. Ko, S.J. Dixon, Protein palmitoylation and cancer, EMBO Rep. 19 (10) (2018), e46666.
[82] V. Rodriguez-Lara, J.M. Hernandez-Martinez, O. Arrieta, Influence of estrogen in non-small cell lung cancer and its clinical implications, J. Thorac. Dis. 10 (1) (2018) 482–497.
[83] D.A. Bachovchin, T. Ji, W. Li, G.M. Simon, J.L. Blankman, A. Adibekian, H. Hoover, S. Niessen, B.F. Cravatt, Superfamily-wide portrait of serine hydrolase inhibition achieved by library-versus-library screening, Proc. Natl. Acad. Sci. U. S. A. 107 (49) (2010) 20941–20946.
[84] L. Abrami, T. Dallavilla, P.A. Sandoz, M. Demir, B. Kunz, G. Savoglidis, V. Hatzimanikatis, F.G. van der Goot, Identification and dynamics of the human ZDHHC16-ZDHHC6 palmitoylation cascade, Elife 6 (2017), e27826.
[85] C. Hedberg, F.J. Dekker, M. Rusch, S. Renner, S. Wetzel, Development of highly potent inhibitors of the ras-targeting human acyl protein thioesterases based on substrate similarity design, Angew Chem. Int. Ed. Engl. 50 (2011) 9832–9837.
[86] D.C. Yeh, J.A. Duncan, S. Yamashita, T. Michel, Depalmitoylation of endothelial nitric-oxide synthase by acyl-protein thioesterase 1 is potentiated by Ca(2+)-calmodulin, J. Biol. Chem. 274 (1999) 33148–33154.
[87] G. Morris, K. Walder, B.K. Puri, M. Berk, M. Maes, The deleterious effects of oxidative and nitrosative stress on palmitoylation, membrane lipid rafts and lipid-based cellular signalling: new drug targets in neuroimmune disorders, Mol. Neurobiol. 53 (7) (2016 Sep) 4638–4658.
[88] V. Rodriguez-Lara, J.M. Hernandez-Martinez, O. Arrieta, Influence of estrogen in non-small cell lung cancer and its clinical implications, J. Thorac. Dis. 10 (1) (2018) 482–497.
[89] X. Gao, Y. Cai, Z. Wang, W. He, S. Cao, R. Xu, H. Chen, Estrogen receptors promote NSCLC progression by modulating the membrane receptor signaling network: a systems biology perspective, J. Transl. Med. 17 (1) (2019) 308. Sep. 11.
[90] T. Smida, T.C. Bruno, L.P. Stabile, Influence of estrogen on the NSCLC microenvironment: a comprehensive picture and clinical implications, Front. Oncol. 10 (2020) 137. Feb 18.
[91] J. Peng, S.I. Meireles, X. Xu, et al., Estrogen metabolism in the human lung: impact of tumorigenesis, smoke, sex and race/ethnicity, Oncotarget 8 (63) (2017) 106778–106789.
[92] B.J. Fuhrman, C. Schairer, M.H. Gail, et al., Estrogen metabolism and risk of breast cancer in postmenopausal women, J Natl Cancer Inst 104 (4) (2012) 326–339, https://doi.org/10.1093/jnci/djr531.
[93] E.L. Cavalieri, D.E. Stack, P.D. Devanesan, R. Todorovic, I. Dwivedy, S. Higginbotham, S.L. Johansson, K.D. Patil, M.L. Gross, J.K. Gooden, R. Ramanathan, R.L. Cerny, E.G. Rogan, Molecular origin of cancer: catechol estrogen-3,4-quinones as endogenous tumor initiators, Proc. Natl. Acad. Sci. U. S. A. 94 (1997) 10937–10942.
[94] J.L. Bolton, G.R. Thatcher, Potential mechanisms of estrogen quinone carcinogenesis, Chem. Res. Toxicol. 21 (2008) 93–101.
[95] L.R. Domingo, M. Rios-Gutierrez, P. Perez, Applications of the conceptual density functional theory indices to organic chemistry reactivity, Molecules 21 (2016).
[96] M.E. Zaballa, F.G. van der Goot, The molecular era of protein S-acylation: spotlight on structure, mechanisms, and dynamics, Crit. Rev. Biochem. Mol. Biol. 53 (4) (2018 Aug) 420–451.
[97] S.J. Won, Cheung see kit M, martin BR. Protein depalmitoylases, Crit. Rev. Biochem. Mol. Biol. 53 (1) (2018) 83–98.
[98] M.O. Parat, R.Z. Stachowicz, P.L. Fox, Oxidative stress inhibits caveolin-1 palmitoylation and trafficking in endothelial cells, Biochem. J. 361 (Pt 3) (2002) 681–688.
[99] Y. Romero, A. Aquino-Gálvez, Hypoxia in cancer and fibrosis: Part of the problem and part of the solution, Int. J. Mol. Sci. 22 (15) (2021) 8335.
[100] K. Skjefstad, T. Grindstad, M.R. Khanehkenari, E. Richardsen, T. Donnem, T. Kilvaer, S. Andersen, R.M. Bremnes, L.T. Busund, S. Al-Saad, Prognostic relevance of estrogen receptor α, β and aromatase expression in non-small cell lung cancer, Steroids 113 (2016) 5–13.
[101] A.L. Titan, H. He, N. Lui, D. Liou, M. Berry, J.B. Shrager, L.M. Backhus, The influence of hormone replacement therapy on lung cancer incidence and mortality, J. Thorac. Cardiovasc. Surg. 159 (4) (2020) 1546–1556.
[102] V. Rodriguez-Lara, M.R. Avila-Costa, An overview of lung cancer in women and the impact of estrogen in lung carcinogenesis and lung cancer treatment, Front. Med. 8 (2021), 600121.
[103] V. Rodriguez-Lara, J.M. Hernandez-Martinez, O. Arrieta, Influence of estrogen in non-small cell lung cancer and its clinical implications, J. Thorac. Dis. 10 (1) (2018) 482–497.
[104] X. Gao, Y. Cai, Z. Wang, W. He, S. Cao, R. Xu, H. Chen, Estrogen receptors promote NSCLC progression by modulating the membrane receptor signaling network: a systems biology perspective, J. Transl. Med. 17 (1) (2019) 308. Sep. 11.